JOURNAL OF MATERIALS SCIENCE 22 (1987) 1432–1436

The effects of external stress on the cubic–tetragonal transformation in rapidly quenched ZrO_2–Y_2O_3

MEZAME SHIBATA, MASAHARU KATO, HIROSHI SETO, TATSUO NOMA*, MASAHIRO YOSHIMURA*, SHIGEYUKI SŌMIYA*
*Department of Materials Science and Engineering, and *Research Laboratory of Engineering Materials, Tokyo Institute of Technology, 4259 Nagatsuta, Midori-ku, Yokohama 227, Japan*

The effects of the external stress on the displacive cubic (c) to tetragonal (t′) transformation, taking place during rapid quenching of ZrO_2–Y_2O_3 alloys by a hammer–anvil unit, were examined through the statistical analysis of the crystallography of the product phases. The initially formed c-phase had no strong texture with respect to the stress direction. However, specific t′ variants among crystallographically equivalent ones were formed preferentially. From these observations, it is concluded that the applied stress plays an important role on the deformation to change the lattice during the c → t′ transformation.

1. Introduction

The ZrO_2–Y_2O_3 system is one of the best investigated systems among the fully stabilized or partially stabilized zirconias. As is well known, this system with less than about 8 mol % Y_2O_3 has three polymorphs as equilibrium solid phases; cubic (c), tetragonal (t) and monoclinic (m) phases. In addition, quenching from the high-temperature c-phase often results in the displacive transformation from c to the metastable tetragonal (t′) phase [1–3]. This transformation is believed to occur in a diffusionless manner and, therefore, the Y_2O_3 content in the t′-phase is usually higher than that in the equilibrium t-phase, although the crystal structures of these two phases are the same.

The diffusionless nature of the c → t′ transformation indicates that there are three crystallographically equivalent t′ variants, depending on which of the three principal axes of the c-phase are converted into the longer axis of the t′-phase. In our previous study, we have examined the microstructures of the rapidly quenched ZrO_2–Y_2O_3 alloys [4]. In the course of the examination, we noticed that the three t′ variants did not necessarily form with equal amounts. Because a hammer–anvil apparatus is used for the rapid quenching from the melts [4], it results in the application of a compressive stress during the c → t′ transformation. If this compressive stress affects the c → t′ transformation in any way, it is then natural to speculate that the formation of specific t′ variants among the crystallographically equivalent ones is aided by the applied stress.

In the present study, the role of the applied stress on the c → t′ transformation will be investigated through the detailed examination of the distribution of the t′ variants in the rapidly quenched ZrO_2–Y_2O_3 alloys.

2. Experimental procedure and results

Thin discs of ZrO_2 alloys, typically 30 to 40 μm thick and 1 to 2 cm diameter, containing 2 to 6 mol % Y_2O_3 were prepared in an arc-imaging furnace by rapid quenching from the melts using a copper-made hammer–anvil apparatus. Specimens suitable for transmission electron microscopy (TEM) were prepared from these discs by the standard ion-milling procedure followed by carbon coating. The TEM observation was made in a 200 kV Hitachi H-700 microscope with a stage of $+/-60°$ tilt and 360° rotation.

All observed specimens had polygonal grains of about 3 μm diameter, as shown in Fig. 1. The X-ray analysis of these specimens revealed that existing phases were t′ and/or c-phases. No m-phase was present. The compositional and structural details of the existing phases will be reported elsewhere [4, 5].

The TEM diffraction pattern analysis has indicated that a single polygonal grain exhibits essentially a unique orientation no matter how complicated is its microstructure. Since the principal axes of the t′-phase are almost parallel to those of the original c-phase [6, 7], the above fact means that the polygonal grains were made at the moment of quenching from the liquid phase to the c-phase. Therefore, the original orientation of the c-phase in any grain upon quenching can be found by observing the as-quenched grains where all or a part of the c-phase has already transformed into the t′-phase.

In order to examine the effect of the external stress on the formation of the c-phase, we performed the following analysis. For each observed grain, the orientation of the specimen surface normal (the compressive stress axis) was examined from a diffraction pattern analysis and it was expressed inside an [0 0 1]–[1 0 1]–[1 1 1] standard triangle of the stereographic projection. Then, for more than 50 grains in alloys with various Y_2O_3 contents, the angles between the stress axis and the [0 0 1], [1 0 1] and [1 1 1] poles were

 0022–2461/87 $03.00 + .12

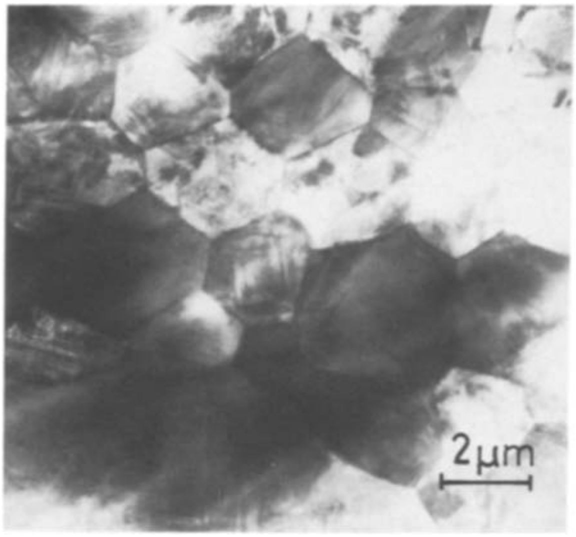

Figure 1 Transmission electron micrograph of rapidly quenched ZrO_2–2.5 mol % Y_2O_3.

measured. The histograms obtained from these measurements are shown in Fig. 2. The calculated probability distributions of the angle appearance on the assumption of the random orientation distribution are also shown in Fig. 2, using dashed lines. The similarity between the calculated curves and the observed histograms leads us to conclude that the external stress does not affect the orientation of the c-phase during the liquid to cubic transformation.

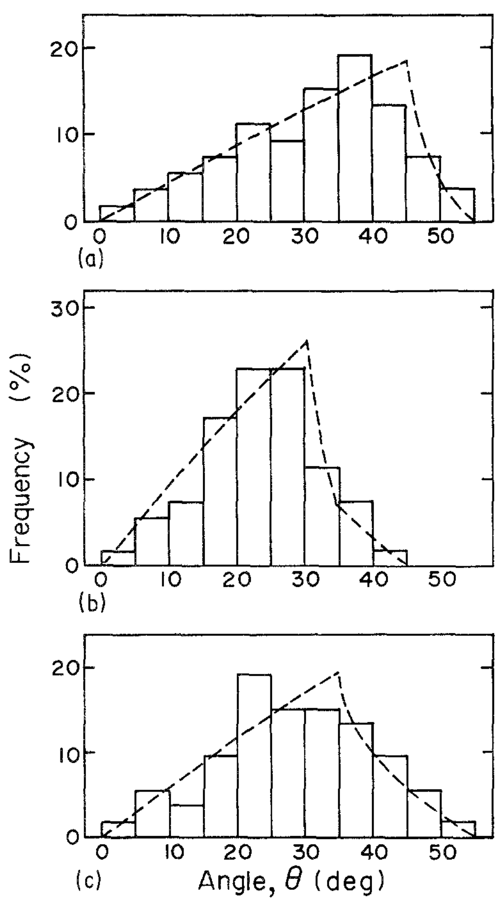

Figure 2 The frequency of appearance (proportional to the number of grains) as a function of the angle between the specimen normal and the (a) [0 0 1], (b) [1 0 1] or (c) [1 1 1] pole of the cubic phase. Note the similarity between the histograms and the calculated probability curves (the dashed lines) on the assumption of random orientation distribution.

Next, we examined the stress effect on the c → t′ transformation as follows. First, the angle θ between the longer axis (c_t) of the t′-phase and the stress axis was measured. In other words, three different θ angles were measured in a grain corresponding to three t′ variants. (Strictly speaking, the principal axes of the t′-phase are not exactly parallel to those of the original c-phase, and therefore, more than three tetragonal variants can be conceived [6]. However, since the deviation is very small (less than 1°) [6], the present simplification is justified.) Secondly, observation of the grain from ⟨1 1 1⟩ zone axes was made to determine the fraction of each of the three t′ variants; the dark-field micrographs, the intensities of the {1 1 2}-type reflection spots and the orientation of the twinning plane in a t′ variant were also used to ascertain whether any specific t′ variants were formed preferentially.

Fig. 3a shows a bright-field image of a ZrO_2–4 mol % Y_2O_3 alloy observed from the [1 1 1] zone axis. This specimen is made entirely of the t′-phase and a complicated twinned structure can be seen. Figs 3b to d show dark-field micrographs of the same area taken, respectively, with one of the three {1 1 2}-type reflection spots of the t′ variants. Fig. 3e shows the stereographic projection of the observed grain orientation with its centre coinciding with the stress axis. With the measurement of the angle θ for each of the t′ variants, we found that $\theta = 75°$ (Fig. 3b), 65° (Fig. 3c) and 29° (Fig. 3d). Because Fig. 3b, taken with the $(1\bar{2}1)$ spot, has the maximum areal fraction of the bright regions, it is found that this particular t′ variant whose c_t-axis is parallel to the [0 1 0] direction of the c-phase, has formed most preferentially, followed in order by Fig. 3c ($c_t \parallel [100]$) and Fig. 3d ($c_t \parallel [001]$). In other words, a t′ variant tends to become more preferentially formed as θ becomes closer to 90°.

Fig. 4 gives another example for a ZrO_2–4.5 mol % Y_2O_3 alloy. In this case, the morphology is simpler and this grain has only two t′ variants which are twin-related with each other. The angles θ of these variants were 85° and 75°. The remaining variant with $\theta = 15°$ could not be found in this grain.

Many different grains in various specimens were statistically examined in this way. The histogram in Fig. 5a summarizes the results of the statistical observation showing the frequency of the appearance of the t′ variants as a function of θ. If there is no correlation between the stress axis and the distribution of the c_t-axis, the observed frequency for the angle range between θ and $\theta + d\theta$ should become proportional to $\sin\theta\, d\theta$. The dashed line shows the sine curve which is normalized so that the area under the curve becomes equal to the total area of the histogram. For easier comparison, the difference Δ between the observed frequency and the normalized sine curve is replotted in Fig. 5b. As can be seen, Δ takes negative values for $\theta < 70°$ and positive values for $\theta > 70°$. From Figs 3, 4 and 5, we conclude that the applied stress makes the formation of the t′ variants easier as θ becomes larger.

3. Discussion

Let us now discuss the effect of the external stress on the c → t′ transformation. As far as we know, no

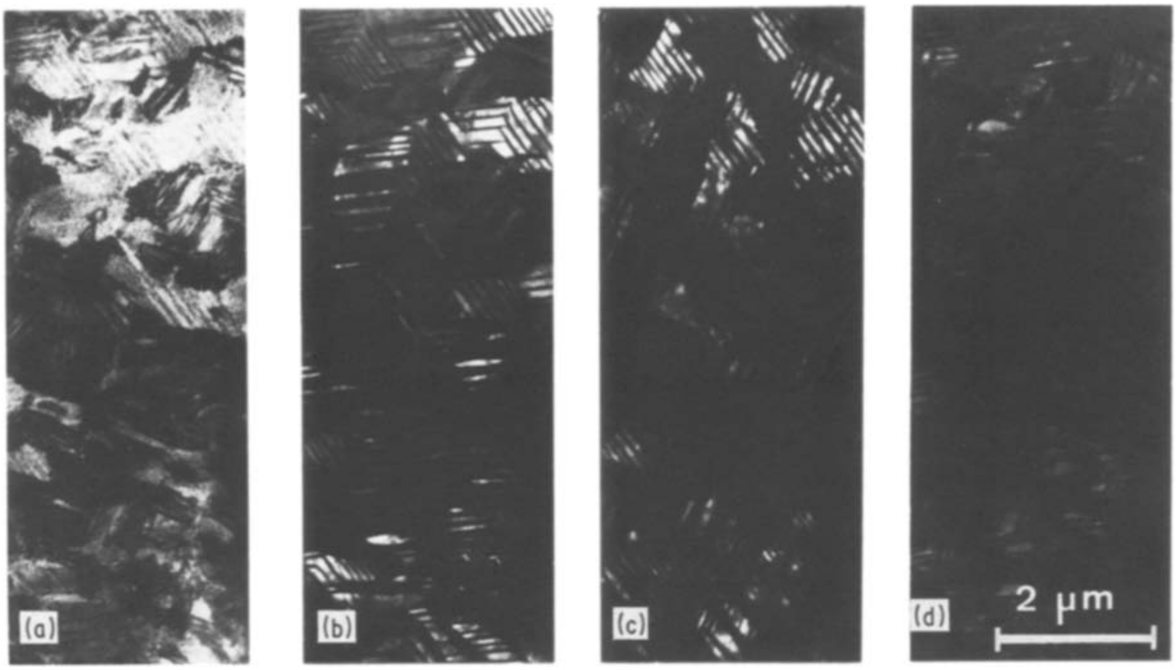

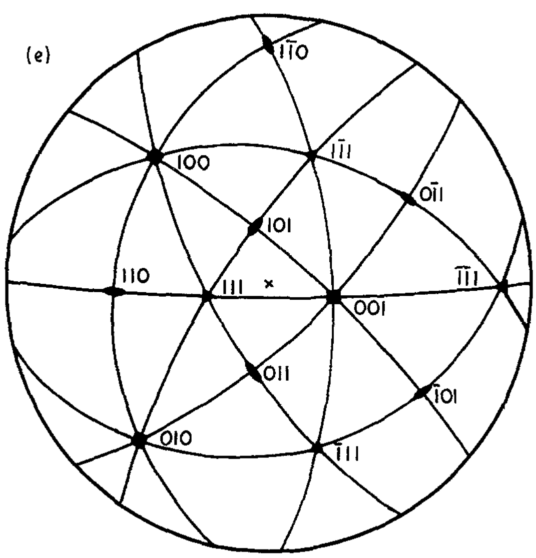

Figure 3 Transmission electron micrographs of the same region in ZrO_2–4 mol % Y_2O_3; (a) bright-field image, (b), (c) and (d) dark-field images taken with three different {1 1 2}-type reflection spots. (e) Stereographic projection showing the orientation of this region.

examination of such a stress effect has been carried out in the ZrO_2–Y_2O_3 system. On the other hand, for metal systems, one can quote many works for the examination of the stress effects on martensitic transformations. In particular, several investigators [8–12] have analysed the preferentially formed stress-induced martensite variants in ferrous alloy single crystals. They have successfully explained the experimental results considering that the applied stress helps the lattice deformation (the Bain deformation) during the initial stage of the transformation. Here, we will examine whether the similar stress effect can be considered for the present system.

The transformation strain for the lattice deformation, ε_{ij}, is written on the Cartesian x_1–x_2–x_3 coordinate system parallel to the principal axes of the parent c-phase as

$$\varepsilon_{ij} = \begin{pmatrix} \varepsilon_1 & 0 & 0 \\ 0 & \varepsilon_1 & 0 \\ 0 & 0 & \varepsilon_2 \end{pmatrix} \qquad (1)$$

for the x_3-axis converting into the c_t-axis. In Equation 1, ε_1 and ε_2 are written in terms of the lattice constants of the $c(a_c)$ and the $t'(a_t$ and c_t, $c_t > a_t)$ phases as

$$\begin{aligned} \varepsilon_1 &= (a_t - a_c)/a_c \\ \varepsilon_2 &= (c_t - a_c)/a_c \end{aligned} \qquad (2)$$

On the other hand, the resolved normal stresses of the uniaxial compressive stress $\sigma(<0)$ can be written as

$$\begin{aligned} \sigma_{11} &= \sigma \cos^2\theta_1 \\ \sigma_{22} &= \sigma \cos^2\theta_2 \\ \sigma_{33} &= \sigma \cos^2\theta_3 \end{aligned} \qquad (3)$$

where $\theta_j (j = 1, 2, 3)$ is the angle between the stress axis and x_j-axis. Then the interaction energy, E_I, per unit volume between σ_{ij} and ε_{ij} becomes,

$$E_I = -\sum_{i=1}^{3}\sum_{j=1}^{3} \sigma_{ij}\varepsilon_{ij} \qquad (4)$$

Substituting Equations 2 and 3 into Equation 4 and noting that $\cos^2\theta_1 + \cos^2\theta_2 + \cos^2\theta_3 = 1$, we have

$$E_I = -\sigma[\varepsilon_1 + (\varepsilon_2 - \varepsilon_1)\cos^2\theta_3]. \qquad (5)$$

Equation 5 indicates that for a given set of lattice constants, E_I depends only on θ_3; the angle between the stress axis and the c_t-axis. (Since the x_3-axis converts into the c_t-axis, the angle θ_3 is identical to the angle θ used in the previous section.) Taking the lattice constants $a_c = 0.5128$, $a_t = 0.5107$ and $c_t = 0.5171$ nm for ZrO_2–4 mol % Y_2O_3 [1], for example, ε_1 and ε_2 become -0.004 and $+0.008$, respectively. Therefore, we have

$$E_I = -\sigma(-0.004 + 0.012\cos^2\theta_3) \qquad (6)$$

Since a negative value of E_I physically means that the external stress can assist the lattice deformation and

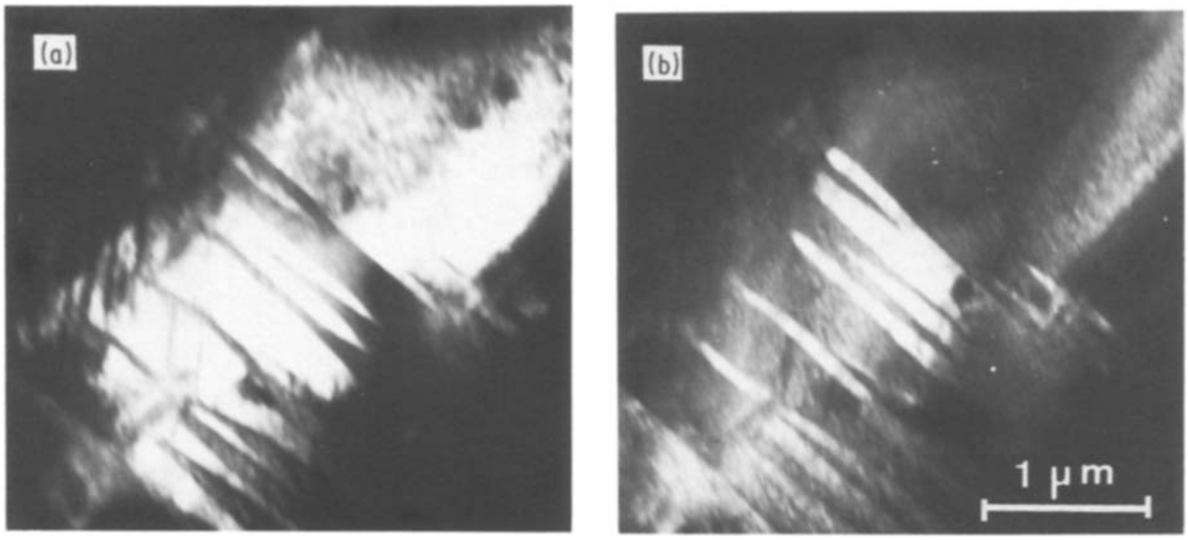

Figure 4 Transmission electron micrographs of ZrO_2–4.5 mol % Y_2O_3; (a) and (b) dark-field images taken with two different {1 1 2}-type reflection spots.

since σ is negative, the above consideration indicates that the formation of a t′ variant with $\theta_3 > 54.7°$ is aided by the external stress and that the closer the c_t-axis of the t′ variant to 90°, the more preferable its formation becomes.

Now we find that the experimental results in Figs 3, 4 and 5 can reasonably be understood through the present analysis; as mentioned in the previous section, the preferentially formed t′ variants are those with large θ values.

A similar analysis can also be applied to the liquid to cubic phase transformation. As shown in Fig. 2, the external stress does not affect the crystallographic orientation of the c-phase. In this case, the transformation strain $\varepsilon_{ij}^{l\to c}$ (the volume change) associated with the transformation from the isotropic liquid phase to the cubic crystal can be written as

$$\varepsilon_{ij}^{l\to c} = \varepsilon\delta_{ij}(\delta_{ij}\text{: Kronecker's delta}) \qquad (7)$$

on any arbitrary Cartesian coordinate system. Here, ε is expressed in terms of the molar volumes of the liquid and c-phases, V_l and V_c, respectively, as $\varepsilon = (V_c - V_l)/3V_l$. Then the interaction energy $E_I^{l\to c}$ per unit volume between the applied stress σ and $\varepsilon_{ij}^{l\to c}$ becomes, from Equations 3 and 7,

$$E_I^{l\to c} = -\sum_{i=1}^{3}\sum_{j=1}^{3}\sigma_{ij}\varepsilon_{ij}^{l\to c} = -\sigma\varepsilon. \qquad (8)$$

In this case, different from the c → t′ transformation, $E_I^{l\to c}$ is independent of the angle θ. Therefore, stress has an effect, which is independent of the orientation of the produced c-phase. Thus, it is reasonable that no preferred orientation was found in the c-phase, although a unidirectional compressive stress was applied during the transformation.

In summary, we conclude that the applied stress helps the lattice deformation of specific t′ variants among crystallographically equivalent ones.

References

1. H. G. SCOTT, *J. Mater. Sci.* **10** (1975) 1527.

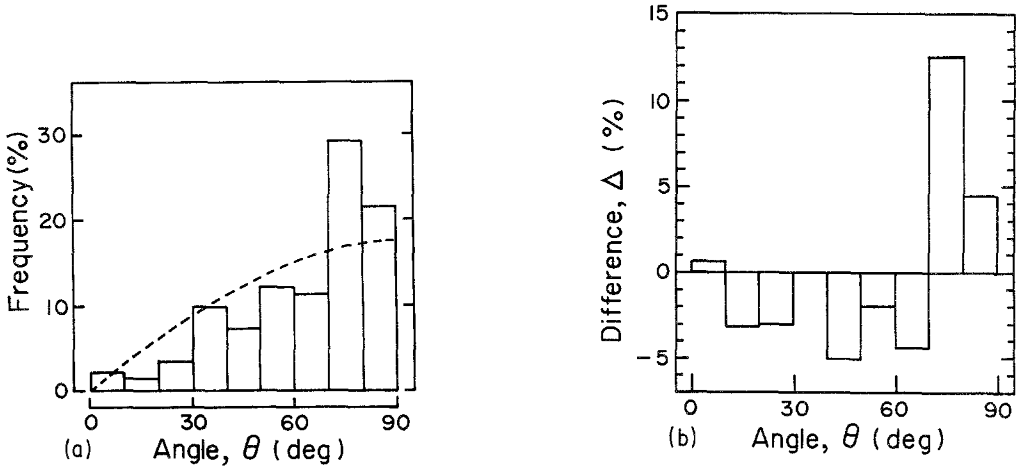

Figure 5 (a) Histogram showing the frequency of appearance (proportional to the volume fraction) of the t′ phase as a function of the angle θ between the specimen surface normal and the longer axis of the tetragonal lattice. The dashed curve expresses the calculated frequency on the assumption of random orientation distribution. (b) Replotting of (a) showing the difference between the observed and calculated frequencies.

2. R. A. MILLER, J. L. SMIALEK and R. G. GARLICK, in "Advances in Ceramics", Vol. 3 (American Ceramic Society, Columbus, Ohio, 1981) p. 241.
3. V. LANTERI, A. H. HEUER and T. E. MITCHELL, *ibid.*, Vol. 12, p. 118.
4. T. NOMA, M. YOSHIMURA, M. KATO, M. SHIBATA, H. SETO and S. SŌMIYA, *J. Amer. Ceram. Soc.*, submitted.
5. *Idem, J. Ceram. Soc. Jpn.* **94** (1986) 887.
6. M. SHIBATA, M. KATO, H. SETO, N. ISHIZAWA, N. MIZUTANI and M. KATO, *J. Amer. Ceram. Soc.*, submitted.
7. N. ISHIZAWA, A. SAIKI, T. YAGI, N. MIZUTANI and M. KATO, *J. Amer. Ceram. Soc.* **69** (1986) C-18.
8. Y. HIGO, F. LECROISEY and T. MORI, *Acta Metall.* **22** (1974) 313.
9. M. KATO and T. MORI, *ibid.* **24** (1976) 853.
10. *Idem, ibid.* **25** (1977) 951.
11. M. KATO, R. MONZEN and T. MORI, *ibid.* **26** (1978) 605.
12. A. SATO, M. KATO, Y. SUNAGA, T. MIYAZAKI and T. MORI, *ibid.* **28** (1980) 367.

Received 2 June
and accepted 18 August 1986